

A Watermark for Auto-Regressive Image Generation Models

Yihan Wu*, Xuehao Cui*, Ruibo Chen, Georgios Milis, Heng Huang

University of Maryland, College Park

ywu42@umd.edu

Abstract

The rapid evolution of image generation models has revolutionized visual content creation, enabling the synthesis of highly realistic and contextually accurate images for diverse applications. However, the potential for misuse, such as deepfake generation, image-based phishing attacks, and fabrication of misleading visual evidence, underscores the need for robust authenticity verification mechanisms. While traditional statistical watermarking techniques have proven effective for autoregressive language models, their direct adaptation to image generation models encounters significant challenges due to a phenomenon we term re-tokenization mismatch—a disparity between original and re-tokenized sequences during the image generation process. To overcome this limitation, we propose C-REWEIGHT, a novel, distortion-free watermarking method explicitly designed for image generation models. By leveraging a clustering-based strategy that treats tokens within the same cluster equivalently, C-REWEIGHT mitigates re-tokenization mismatch while preserving image fidelity. Extensive evaluations on leading image generation platforms reveal that C-REWEIGHT not only maintains the visual quality of generated images but also improves detectability over existing distortion-free watermarking techniques, setting a new standard for secure and trustworthy image synthesis.

1 Introduction

Auto-regressive image generation models, which power cutting-edge visual synthesis applications, have made remarkable strides in producing highly realistic and context-aware images. As these models are increasingly integrated into diverse platforms—from content creation and digital art to real-time visual augmentation—their potential for misuse also grows. Malicious actors can exploit

these technologies to fabricate convincing visual evidence, generate deepfake imagery for misinformation, or automate phishing schemes with manipulated visuals. Moreover, the proliferation of synthetic images threatens the authenticity of digital media and raises concerns in legal scenarios where image verification is critical. To mitigate these risks, embedding robust and detectable watermarks in auto-regressive image outputs is crucial, ensuring traceability and accountability while protecting against unauthorized manipulation and misuse.

Statistical watermarking techniques have emerged as a promising solution for identifying machine-generated content from autoregressive language models (Kirchenbauer et al., 2023). However, extending these methods directly to autoregressive image generation models faces a critical challenge known as re-tokenization mismatch. Unlike their language-based counterparts, autoregressive image models involve an additional encoding and decoding phase. During image synthesis, the initial image prompt is first transformed into a sequence of discrete tokens through an encoder. This token sequence is then processed using next-token prediction to generate an output sequence, which is finally decoded back into image form. To verify the presence of a watermark, the generated image must be re-encoded into its tokenized representation. However, the re-encoded token sequence often deviates from the original one used for generation, resulting in re-tokenization mismatch. This inconsistency severely hampers the effectiveness of traditional watermarking methods when applied directly to image models.

To overcome this limitation, we propose C-REWEIGHT, a novel, distortion-free watermarking technique specifically crafted for autoregressive image generation models. Our key insight is that mismatched token pairs between the original and re-encoded sequences display a higher degree of

*Equal contribution.

similarity compared to random token pairs. Capitalizing on this observation, we design a clustering-based watermarking framework that treats tokens within the same cluster as equivalent, effectively mitigating the impact of retokenization mismatch.

We summarize our contributions as follows:

- We propose C-REWEIGHT, a novel distortion-free watermarking framework explicitly designed to address the unique challenges posed by autoregressive image generation models. Unlike traditional statistical watermarking techniques, C-REWEIGHT effectively mitigates the impact of retokenization mismatch through a clustering-based strategy, ensuring consistent watermark detectability even after image decoding and re-encoding.
- We introduce a clustering-based equivalence mechanism that leverages token similarity to enhance watermark resilience. By grouping tokens with high similarity into clusters, our method preserves watermark signals across retokenization processes without altering image fidelity, enabling reliable verification.
- We perform comprehensive evaluations on state-of-the-art autoregressive image generation models, demonstrating that C-REWEIGHT consistently outperforms existing watermarking methods. Experimental results reveal a 10% increase in detection accuracy, establishing a new benchmark for robustness and reliability in watermarking synthetic images.

2 Related Work

Auto-regressive generative models. Auto-regressive models have played a pivotal role in advancing language modeling, powering state-of-the-art systems such as GPT-3 and ChatGPT (Vaswani et al., 2017; Raffel et al., 2020; Brown, 2020), and prompting discourse on the emergence of artificial general intelligence. In multimodal domains, however, image generation has been predominantly driven by diffusion-based approaches (e.g., Stable Diffusion (Rombach et al., 2022)), while vision-language understanding has relied on compositional frameworks like CLIP (Radford et al., 2021) paired with LLMs (e.g., LLaVA (Liu et al., 2023)). Attempts to unify generation and perception, such as Emu (Sun et al., 2023) and Chameleon (Team, 2024), either depend on coupling LLMs with diffusion models

or fall short of matching the task-specific performance of specialized methods. More recently, Emu3 (Wang et al., 2024) demonstrates that a unified auto-regressive model trained purely via next-token prediction can achieve state-of-the-art results across vision, language, and video tasks. By tokenizing all modalities into a shared discrete space, Emu3 trains a single transformer from scratch on a diverse mix of multimodal sequences, bypassing the need for diffusion processes or compositional fusion techniques.

Diffusion model watermarking. Diffusion model watermarking embeds watermarks directly during the image generation process to ensure minimal perceptual distortion. Some techniques achieve this by modifying the generative model itself, for instance, by fine-tuning specific components, as seen in Stable Signature (Fernandez et al., 2023). Alternatively, other methods embed watermarks by perturbing the initial noise input, avoiding the need for extensive model retraining. Tree-Ring (Wen et al., 2023), for example, inserts a Fourier-domain pattern into the initial noise, which can be recovered via DDIM inversion (Song et al., 2020). RingID (Ci et al., 2024) extends this approach to support multiple watermark keys. Additional notable techniques include Gaussian Shading (Yang et al., 2024), which generates a unique key per watermark owner, and PRC (Gunn et al., 2024), which employs pseudo-random error-correcting codes to achieve computationally undetectable watermarking. These approaches are orthogonal to our work, as they are specifically tailored for diffusion models and cannot be readily applied to other generative architectures.

Distortion-free watermark. (Aaronson, 2022) introduced a pioneering distortion-free watermarking method that leverages Gumbel-Softmax to adjust token distributions without altering content quality. Building on this concept, (Christ et al., 2023) and (Kuditipudi et al., 2023) applied inverse-sampling and Gumbel-Softmax techniques, respectively, to modify token distributions in watermarked outputs. Their approaches rely on watermark keys derived from either token positions or predefined key lists. However, (Christ et al., 2023)’s method demonstrates limited robustness against modifications and lacks empirical validation of its detectability. In contrast, (Kuditipudi et al., 2023)’s approach necessitates substantial resampling from the secret key distri-

bution for effective detection, resulting in inefficiencies for long-form content. To address these limitations, (Hu et al., 2023) introduced inverse-sampling and reweight strategies, although their detection mechanism is not model-agnostic and depends on access to the language model API and specific prompts. Subsequently, (Wu et al., 2023) enhanced the reweighting approach and proposed a model-agnostic detection method. Most recently, (Dathathri et al., 2024) introduced SynthID, achieving distortion-free watermarking for LMs across multiple generations, advancing scalability and detection robustness.

3 Preliminary

Notations. We follow the notations used in (Hu et al., 2023). The vocabulary (or token) set is denoted by V and its cardinality by $N = |V|$. We define the set \mathcal{V} , which includes all possible token sequences including those of zero length and the set \mathcal{A} , which includes all possible images. Within an autoregressive image generation model, a token sequence is generated based on a specific prompt. At any given step, the probability of producing the next token $x_{n+1} \in V$, given the preceding sequence x_1, \dots, x_n , is denoted by $P_M(x_{n+1} | x_1, x_2, \dots, x_n)$. For simplicity and clarity, we adopt a more concise notation: $P_M(x_{n+1:n+m} | x_{1:n})$, where $x_{n+1:n+m} = (x_{n+1}, \dots, x_{n+m})$. It is important to note that the prompt is intentionally excluded from this notation. In image generation models, we denote the image-token encoder by $E(\cdot) : \mathcal{A} \rightarrow \mathcal{V}$ and the token-image decoder by $D(\cdot) : \mathcal{V} \rightarrow \mathcal{A}$.

3.1 Statistical Watermarks

In watermarking applications, the service provider employs a set of *i.i.d.* watermark codes $\{\theta_i \in \Theta, i \in \mathbb{N}\}$, defined over the code space Θ . Each code θ_i is typically derived from a secret key $\text{key} \in \mathcal{K}$ and the n-gram preceding context, denoted $\mathbf{x}_{t-n:t-1}$.

In the watermark generator, a reweight strategy is used to embed a statistical signal into the generated content. Let \mathcal{P} denote the set of all probability distributions over the token set V . The reweight strategy is a function $P_W : \mathcal{P} \times \Theta \rightarrow \mathcal{P}$. For the token distribution at the $(n+1)$ -th generation step, $P_M(x_{n+1} | \mathbf{x}_{1:n}) \in \mathcal{P}$, the watermarked distribution is defined by $P_W(P_M(x_{n+1} | \mathbf{x}_{1:n}), \theta_i)$. For brevity, this is represented as $P_W(x_{n+1} | \mathbf{x}_{1:n}, \theta_i)$.

A distortion-free watermark ensures that the averaged distribution $P_W(x_{n+1} | \mathbf{x}_{1:n}, \theta_i)$ with respect to θ_i is equal to the original distribution $P_M(x_{n+1} | \mathbf{x}_{1:n})$.

Definition 3.1 (Distortion-free watermark). Given the watermark code set Θ , a distribution \mathcal{P}_Θ on Θ , original LM distribution P_M , and the watermarked distribution $P_W(\cdot | \theta \in \Theta)$ A distortion-free watermark should satisfy $\forall x \in V$,

$$\mathbb{E}_{\theta \sim \mathcal{P}_\Theta} [P_W(x | \mathbf{x}_{1:n}, \theta)] = P_M(x | \mathbf{x}_{1:n}).$$

Current popular distortion-free strategies include Gumbel-softmax (Aaronson, 2022), inverse-sampling (Christ et al., 2023; Hu et al., 2023; Kudiptudi et al., 2023) and reweight-based strategy (Wu et al., 2023; Dathathri et al., 2024).

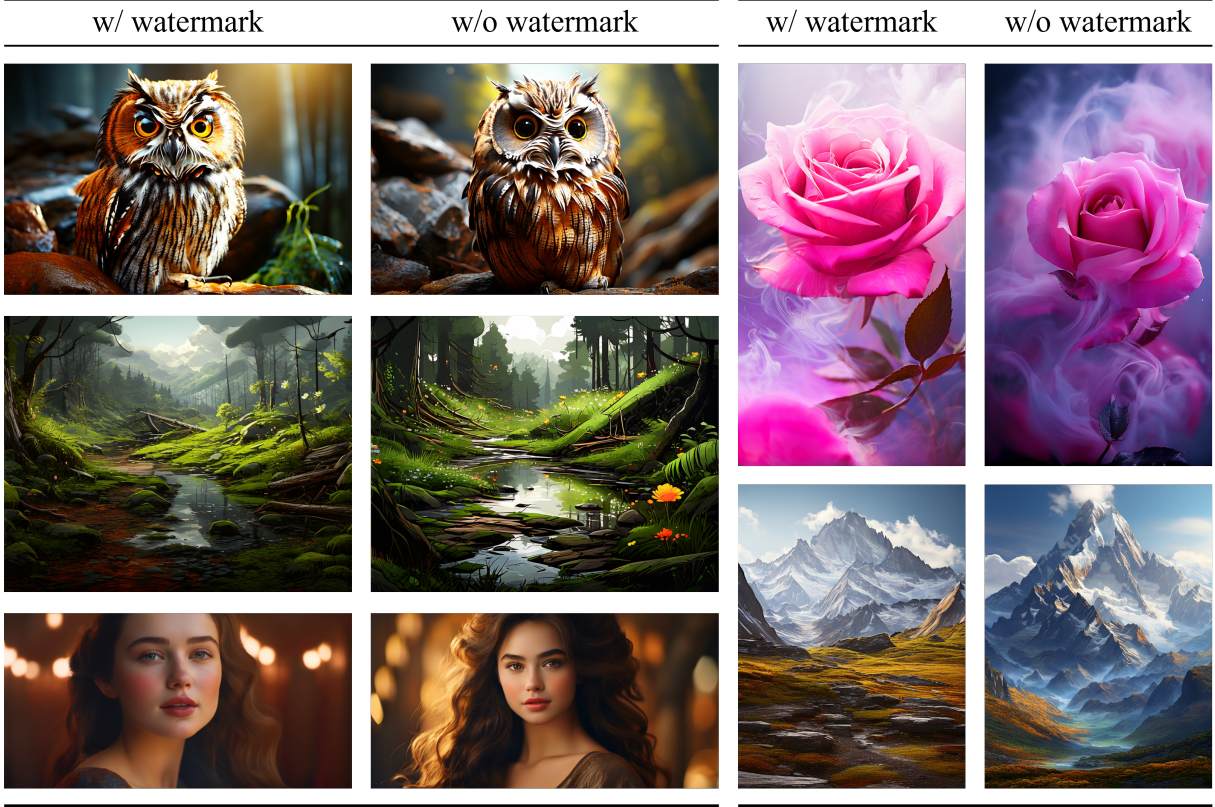
During watermark detection, the user only has access to the watermark key, the reweight strategy, and the generated image. The detector employs a hypothesis testing approach to ascertain the presence of the watermark signal. The null hypothesis H_0 is defined as “*The content is generated without the presence of watermarks*”. The detector adopts a score function based on the watermark key and the reweight strategy, which exhibits statistical bias between the watermarked and unwatermarked token sequences.

3.2 Autoregressive image generation models

The vision tokenizer of Emu3 is trained based on SBER-MoVQGAN (Zheng et al., 2022), which can encode a $4 \times 512 \times 512$ video clip or a 512×512 image into 4096 discrete tokens from a codebook of size 32,768. The tokenizer achieves $4\times$ compression in the temporal dimension and 8×8 compression in the spatial dimension, applicable to any temporal and spatial resolution. Building on the MoVQGAN architecture (Zheng et al., 2022), we incorporate two temporal residual layers with 3D convolution kernels into both the encoder and decoder modules to enhance video tokenization capabilities. The tokenizer is trained end-to-end on the LAION-High-Resolution image dataset (Schuhmann et al., 2022) and the InternVid (Wang et al., 2023) video dataset using combined objective functions of L2 loss, LPIPS perceptual loss (Zhang et al., 2018), GAN loss, and commitment loss (Esser et al., 2021).

Retokenization mismatch. Let \mathbf{x} represent the output token sequence of the image generation model, where the output image is decoded through

Table 1: Visual Comparison of generation results with and without C-REWEIGHT.



the image-token decoder $D(x)$. During watermark detection, the generated image is re-encoded through the encoder $E(D(x))$, and the watermark signal within $E(D(x))$ is detected via a hypothesis test. However, there is typically a discrepancy between $E(D(x))$ and x , which can diminish the statistical signal introduced by the detection scores. We can interpret this as an inevitable token-level edit attack during detection.

4 Methodology

To mitigate retokenization mismatches in autoregressive image generators, we propose C-REWEIGHT, a clustering-based watermarking framework. First, the discrete image tokens are grouped into clusters. On top of these clusters we design a distortion-free, cluster-specific reweighting rule that perturbs the model’s output probabilities only at the cluster level. During generation, this rule steers sampling so that each emitted token lies in the cluster dictated by the secret watermark code; during detection, we simply test whether the recovered token belongs to the prescribed cluster. Because a retokenization error usually maps a token to another member of the same cluster, the detector still receives a reliable statistical signal.

Algorithm 1 Cluster-based reweight.

- 1: **Input:** Original model distribution $P_M(\cdot|\mathbf{x}_{1:n})$. Watermark code θ .
 - 2: Calculate cluster probabilities $\Pr(c_i) := \sum_{x \in c_i} P_M(x|\mathbf{x}_{1:n}), i \in [h]$.
 - 3: Calculate distribution $\mathcal{P}_c := \text{norm}(\min\{0, h \Pr(c_i) - 1\}, \dots, \min\{0, h \Pr(c_i) - 1\})$.
 - 4: Pseudo-randomly select a cluster $c_{i'(\theta)}$.
 - 5: Randomly select $j \sim \text{Uniform}([0, 1])$.
 - 6: **if** $j < \Pr(c_{i'(\theta)})$ **then**
 - 7: $c_{i(\theta)} = c_{i'(\theta)}$
 - 8: **else**
 - 9: Sampling $c_{i''(\theta)} \sim \mathcal{P}_c$.
 - 10: $c_{i(\theta)} = c_{i''(\theta)}$
 - 11: Sampling next token x via Eq. 1.
 - 12: **return** x .
-

The remainder of this section is organized as follows. We begin by describing the clustering procedure and the accompanying cluster-based reweight strategy that preserves distortion while counteracting retokenization errors. We then present the generic watermarking algorithm built on this strategy, together with its associated detection statistic.

4.1 Cluster-based reweight strategy

Image token clustering. In image token clustering, the objective is to split all image tokens into distinct clusters based on their similarity. It is crucial to note that the clustering algorithm is executed only once for each image generation model. After the clusters have been established, there is no need to rerun the algorithm during watermark generation and detection. Consequently, this approach does not significantly increase computational costs. To achieve this, we collect the image token embeddings $\{e_1, \dots, e_m\}$ based on the token-image decoder D and use k-means algorithm to generate the corresponding clusters $\{c_1, \dots, c_h\}$. With the above-mentioned segmentation strategy, mismatched tokens are more likely to be in the same cluster because they are supposed to share similar embeddings in the decoder D . The watermark generator and detector can utilize the cluster information to avoid the detectability reduction caused by the retokenization mismatch. The inverse sampling watermark is a distortion-free method that can be applied directly to clustering scenarios.

DiP-reweight. DiP-reweight (Wu et al., 2023) is a representative example of a two-cluster distortion-free reweighting strategy. In DiP-reweight, the token set is partitioned into two clusters: a red list and a green list. The method aims to promote the total probability mass of the green tokens. Specifically, token probabilities are arranged along the interval $[0, 1]$, with red tokens placed at the beginning and green tokens at the end. To achieve distortion-free watermarking, a parameter $\alpha \leq 0.5$ is selected such that probabilities in $[0, \alpha]$ are removed, those in $[\alpha, 1 - \alpha]$ remain unchanged, and those in $[1 - \alpha, 1]$ are doubled. However, DiP-reweight is restricted to two-cluster settings, limiting its applicability in scenarios involving multiple clusters. To overcome this limitation, we propose a novel cluster-based reweighting strategy tailored for multi-cluster settings.

Cluster-based reweight. Denote by the token clusters $\{c_1, \dots, c_h\}$. Given the preceding tokens $\mathbf{x}_{1:n}$, the cluster-based reweight consists of two steps. In the first step, we pseudo-randomly select a token cluster $c_{i(\theta)}$ (with equal probability) based on the watermark code θ through reject sampling. In the second step, we randomly sample a token from $c_{i(\theta)}$ based on the original model’s distribution.

For the first step, we will first calculate

Algorithm 2 C-REWEIGHT generator.

- 1: **Input:** secret key **key**, prompt $\mathbf{x}_{-m:0}$, generate length $t \in \mathbb{N}$, token-image decoder D .
 - 2: Initialize watermark code history $hist$.
 - 3: **for** $i = 1, \dots, t$ **do**
 - 4: Calculate the token distribution for generating the i -th token $P_M(\cdot | \mathbf{x}_{-m:i-1})$.
 - 5: Generate a watermark code $\theta_i = (\mathbf{key}, \mathbf{x}_{i-n,i-1})$.
 - 6: **if** $\theta_i \in hist$ **then**
 - 7: Sample the next token x_i using distribution
 - 8: **else**
 - 9: Generate the pseudo-random number $r(\theta_i)$.
 - 10: Calculate watermarked distribution $P_W(\cdot | \mathbf{x}_{-m:i-1})$ via cluster-based reweight.
 - 11: Sample the next token x_i using distribution $P_W(\cdot | \mathbf{x}_{-m:i-1})$.
 - 12: **return** image $D(\mathbf{x}_{1:t})$.
-

the cluster probabilities $\Pr(c_1), \dots, \Pr(c_h)$ via $\Pr(c_i) := \sum_{x \in c_i} P_M(x | \mathbf{x}_{1:n})$. We will first pseudo-randomly selected a cluster $c_{i'(\theta)}$ based on the watermark code θ . Then we randomly select a number $j \in [0, 1]$, if $j < h \Pr(c_{i'(\theta)})$, we will sample a token within $c_{i'(\theta)}$. Otherwise, we reject this sample and sample another cluster $c_{i''(\theta)}$ based on the overflow probability distribution $\mathcal{P}_c := norm(\min\{0, h \Pr(c_i) - 1\}, \dots, \min\{0, h \Pr(c_i) - 1\})$, where $norm$ is a distribution normalization function.

Given the selected cluster $c_{i(\theta)}$, in the second step we randomly sample a token from $c_{i(\theta)}$ based on the original model’s token probability, i.e.,

$$P_W(x | \mathbf{x}_{1:n}, \theta) := \begin{cases} \frac{P_M(x | \mathbf{x}_{1:n})}{\Pr(c_{i(\theta)})}, & \text{if } x \in c_{i(\theta)} \\ 0, & \text{if } x \notin c_{i(\theta)}. \end{cases} \quad (1)$$

Details on this method are in Algorithm 1.

Theorem 4.1. *Cluster-based reweight is distortion-free.*

The detailed proof can be found in Appendix A

With the aforementioned probability assignments, we can define a statistical score for the detector based on the watermark code θ and the current token x .

Definition 4.2. Given the watermark code θ and the current token x , the detection score $s(\theta, x)$ is

Table 2: Detectability comparison with KGW (Kirchenbauer et al., 2023), Unigram (Hu et al., 2023) and DiPmarkk (Wu et al., 2023) on Pickapic_v2 (Kirstain et al., 2023), MSCOCO (Lin et al., 2014), Flickr8k (Hodosh et al., 2013) and LAION (Schuhmann et al., 2022) datasets. [**KEY**: best]

Dataset	Pickapic_v2		MSCOCO		Flickr8k		LAION	
FPR	1%	0.1%	1%	0.1%	1%	0.1%	1%	0.1%
KGW($\delta=0.5$)	0.31	0.13	0.34	0.15	0.48	0.22	0.24	0.10
KGW($\delta=1.0$)	0.75	0.53	0.75	0.52	0.80	0.68	0.75	0.49
KGW($\delta=1.5$)	0.92	0.77	0.92	0.82	0.96	0.94	0.89	0.79
KGW($\delta=2.0$)	0.94	0.91	0.95	0.93	0.97	0.95	0.95	0.88
Unigram($\delta=0.5$)	0.79	0.59	0.82	0.65	0.85	0.78	0.83	0.65
Unigram($\delta=1.0$)	0.96	0.86	0.94	0.88	0.99	0.97	0.93	0.86
Unigram($\delta=1.5$)	0.97	0.96	0.99	0.98	0.99	0.98	0.98	0.97
Unigram($\delta=2.0$)	0.99	0.96	0.99	0.99	0.99	0.99	0.98	0.98
ITS-edit	0.51	0.41	0.43	0.34	0.59	0.53	0.56	0.43
EXP-edit	0.94	0.92	0.93	0.90	0.95	0.94	0.93	0.92
γ -reweight	0.44	0.31	0.51	0.35	0.51	0.38	0.45	0.23
DiPmark($\alpha=0.4$)	0.24	0.12	0.36	0.16	0.52	0.34	0.25	0.09
DiPmark($\alpha=0.3$)	0.16	0.05	0.15	0.06	0.26	0.10	0.09	0.04
STA-1	0.24	0.09	0.25	0.12	0.20	0.07	0.21	0.07
C-REWEIGHT($h=100$)	0.96	0.94	0.99	0.99	0.99	0.95	0.99	0.99
C-REWEIGHT($h=200$)	0.99	0.98	0.99	0.99	0.99	0.98	0.99	0.98

Algorithm 3 C-REWEIGHT detector.

- 1: **Input:** image a , image-token encoder E , secret key key , score function s , threshold z .
- 2: calculate token sequence $\mathbf{x}_{1:t} = E(a)$
- 3: Initialize the score function: $S = 0$.
- 4: **for** $i = 2, \dots, t$ **do**
- 5: Generate the watermark code $k_i = (\text{key}, \mathbf{x}_{i-n, i-1})$.
- 6: Generate the pseudo-random number $r(\theta_i)$.
- 7: Update the score function via $S = S + s(\theta_i, x_i)$.
- 8: **return** $S > z$.

defined as

$$s(\theta, x) := \begin{cases} 1 & \text{if } x \in c_{i'(\theta)}, \\ 0 & \text{otherwise.} \end{cases} \quad (2)$$

Note, when $\Pr(c_{i'(\theta)}) < \frac{1}{h}$, cluster-based reweight may sample tokens from clusters other than $c_{i'(\theta)}$. This can reduce detection accuracy. However, empirical results indicate that the overall detectability of cluster-based reweight still sur-

passes that of the state-of-the-art distortion-free reweight strategy.

4.2 C-REWEIGHT

Leveraging the cluster-based reweight strategy, we design our watermarking scheme, C-REWEIGHT, which contains two main components: a *watermark generator* and a *watermark detector*.

Watermark generator. At generation step t , a watermark code θ_t is derived from the secret key key and the n -gram context $\mathbf{x}_{t-n, t-1}$. This code first selects a reference cluster $c_{i'(\theta_t)}$. Following the reweight rule, the actual sampling cluster $c_{i(\theta_t)}$ is chosen using the original cluster probability $\Pr(c_{i'(\theta_t)})$ and the overflow distribution \mathcal{P}_c . The next token x_t is then sampled from $c_{i(\theta_t)}$ according to the base model distribution $P_M(\cdot | \mathbf{x}_{1:t-1})$. To preserve distortion-freeness across multiple generations, we adopt the watermark-code history *hist* of (Hu et al., 2023): whenever $\theta_t \in \text{hist}$, we revert to sampling directly from the unmodified model distribution. The full procedure is given in Alg. 2.

Watermark detector. Detection assumes access to the generated image and the same key key . The

Table 3: Robustness comparison on detectability under l_2 noise attacks. [**KEY**: best]

Budget	l_2		
	0.25	0.50	1.00
KGW($\delta=0.5$)	0.26	0.24	0.24
KGW($\delta=1.0$)	0.60	0.65	0.69
KGW($\delta=1.5$)	0.81	0.79	0.80
KGW($\delta=2.0$)	0.94	0.94	0.94
Unigram($\delta=0.5$)	0.78	0.61	0.55
Unigram($\delta=1.0$)	0.92	0.88	0.87
Unigram($\delta=1.5$)	0.97	0.97	0.96
Unigram($\delta=2.0$)	0.99	0.96	0.97
ITS-edit	0.34	0.39	0.43
EXP-edit	0.88	0.89	0.88
γ -reweight	0.36	0.38	0.35
DiPmark($\alpha=0.4$)	0.22	0.22	0.23
DiPmark($\alpha=0.3$)	0.12	0.13	0.08
STA-1	0.21	0.20	0.22
C-REWEIGHT($h=200$)	0.99	0.99	0.99

Table 4: Robustness comparison on detectability under l_∞ noise attacks. [**KEY**: best]

Budget	l_∞		
	2/255	4/255	8/255
KGW($\delta=0.5$)	0.15	0.06	0.06
KGW($\delta=1.0$)	0.48	0.17	0.13
KGW($\delta=1.5$)	0.64	0.35	0.14
KGW($\delta=2.0$)	0.68	0.39	0.19
Unigram($\delta=0.5$)	0.70	0.62	0.47
Unigram($\delta=1.0$)	0.90	0.79	0.59
Unigram($\delta=1.5$)	0.97	0.84	0.72
Unigram($\delta=2.0$)	0.95	0.90	0.79
ITS-edit	0.17	0.02	0.01
EXP-edit	0.74	0.55	0.33
γ -reweight	0.21	0.08	0.05
DiPmark($\alpha=0.4$)	0.12	0.05	0.01
DiPmark($\alpha=0.3$)	0.07	0.05	0.02
STA-1	0.17	0.06	0.03
C-REWEIGHT($h=200$)	0.93	0.91	0.78

image encoder E recovers the token sequence $\mathbf{x}_{1:t}$. For each position $i = 1, \dots, t$, we recompute the code θ_i from the key and local n -gram context, then evaluate the detection statistic $s(\theta_i, x_i)$ from Definition 4.2. The aggregate statistic is

$$S(\mathbf{x}_{1:t}) = \sum_{i=1}^t s(\theta_i, x_i),$$

and Alg. 3 lists the full algorithm.

Statistical test. Under the null hypothesis (no watermark), $S(\mathbf{x}_{1:t})$ follows a binomial distribution with success probability $\frac{1}{h}$, yielding the tail bound

$$\Pr(S(\mathbf{x}_{1:t}) \geq k) = \sum_{i=\lceil k \rceil}^t \binom{t}{i} \left(\frac{1}{h}\right)^i \left(\frac{h-1}{h}\right)^{t-i}.$$

5 Experiments

We implemented our pipeline in Python using the PyTorch framework and conducted experiments on four NVIDIA GeForce H100 GPUs. The experiments were performed on four datasets: Pickapic_v2 (Kirstain et al., 2023), MSCOCO (Lin et al., 2014), Flickr8k (Hodosh et al., 2013), and LAION (Schuhmann et al., 2022). We followed the generation configurations provided by each dataset, except that the generated images vary in size and

aspect ratio. The auto-regressive image generation models for image generation and evaluation of the effectiveness of our proposed C-REWEIGHT are Emu3 (Wang et al., 2024) models.

Baselines and parameters. We evaluate the performance of our methods by comparing them with multiple baseline approaches, which include two biased watermarking methods, i.e., KGW (Kirchenbauer et al., 2023) and Unigram (Zhao et al., 2023), as well as five unbiased watermarking algorithms, i.e., ITS-edit (Kuditipudi et al., 2023), EXP-edit (Kuditipudi et al., 2023), γ -reweight (Hu et al., 2023), DiPmark (Wu et al., 2023), and STA-1 (Mao et al., 2024). For DiPmark, we choose $\alpha \in \{0.3, 0.4\}$. For the KGW watermark (Kirchenbauer et al., 2023), we use $\delta \in \{0.5, 1.0, 1.5, 2.0\}$ and $\gamma = 0.5$. For Unigram (Zhao et al., 2023), we select $\delta \in \{0.5, 1.0, 1.5, 2.0\}$. The parameters for ITS-edit (Kuditipudi et al., 2023), EXP-edit (Kuditipudi et al., 2023), γ -reweight (Hu et al., 2023), and STA-1 (Mao et al., 2024) are taken directly from their original papers. We generate 500 examples for each task. The watermark keys are constructed using the prefix 1-gram combined with a secret key.

5.1 Detectability

We evaluate the detectability of C-REWEIGHT on the image generation task against baselines in Ta-

Table 5: Quantitative measurement of generated images.

	Pickapic_v2		MSCOCO		Flickr8k		LAION	
	FID↓	CLIP↑	FID↓	CLIP↑	FID↓	CLIP↑	FID↓	CLIP↑
w/o watermark	162.06	0.854	136.41	0.872	153.18	0.870	112.36	0.906
ITS-edit	163.02	0.857	136.00	0.875	149.76	0.861	117.11	0.906
EXP-edit	151.17	0.850	140.61	0.868	151.55	0.862	118.11	0.902
γ -reweight	154.03	0.862	140.72	0.867	150.46	0.861	116.91	0.906
DiPmark($\alpha=0.4$)	148.97	0.863	141.12	0.860	150.52	0.864	118.46	0.901
DiPmark($\alpha=0.3$)	153.32	0.862	139.00	0.865	150.04	0.861	114.95	0.905
STA-1	155.15	0.864	132.26	0.873	151.03	0.870	117.96	0.906
C-REWEIGHT($h=200$)	155.16	0.865	129.21	0.872	138.28	0.868	109.19	0.909

ble 2. Following the evaluation metric of the previous works (Kirchenbauer et al., 2023; Wu et al., 2023), we report the True Positive Rate (TPR) at guaranteed False Positive Rates (FPR), i.e., $\text{TPR@FPR}=\{1\%, 0.1\%\}$. Notice that since the detectors for ITS-edit and EXP-edit lack a theoretical guarantee, we follow their original settings and report the true positive rate at their empirical false positive rate. Our method outperforms all other unbiased watermarks, showcasing superior detectability across different datasets.

5.2 Robustness

We assess the robustness of the image watermark against various noise attacks, as presented in Table 3 and 4. Specifically, we apply l_2 noise with budgets $\{0.25, 0.50, 1.00\}$ and l_∞ noise with budgets $\{2/255, 4/255, 8/255\}$ to simulate different attack scenarios. The detectability of each watermark is tested on images generated using the configuration of the Pickapic_v2 (Kirstain et al., 2023) dataset. We use True Positive Rate at a fixed False Positive Rate of 1% ($\text{TPR@FPR}=1\%$) as the evaluation metric. The results demonstrate that C-REWEIGHT consistently outperforms all other unbiased watermarking methods under these adversarial conditions, highlighting its superior robustness to noise attacks. This performance underscores its effectiveness in maintaining detectability even when subjected to significant perturbations.

5.3 Image Quality

Qualitative Comparison We present a qualitative comparison of generation results in Table 1. Each pair of images is generated under identical settings, including the prompt and image size. The results indicate that images generated with C-

REWEIGHT exhibit no noticeable degradation in visual quality compared to those produced without watermarking.

Quantitative Evaluation For unbiasedness validation, we compute the Fréchet Inception Distance (FID) score (Heusel et al., 2017) and the CLIP score (Radford et al., 2021) between watermarked and unwatermarked images generated from the same prompts. The FID score measures the distance between feature vectors extracted using Inception models, while the CLIP score quantifies the cosine similarity between image embeddings. We use the scores between two sets of unwatermarked images as baseline. The results demonstrate that images watermarked with C-REWEIGHT maintain comparable quality to their unwatermarked counterparts, as evidenced by the similarity in FID and CLIP scores. This confirms that C-REWEIGHT effectively preserves image quality while embedding a watermark.

6 Conclusion

We introduce C-REWEIGHT, a novel distortion-free watermarking method specifically designed for autoregressive image generation. By employing a clustering-based strategy that accounts for token similarity during retokenization, C-REWEIGHT effectively mitigates sequence mismatches while preserving image fidelity. Experimental evaluations confirm that C-REWEIGHT not only maintains the visual quality of generated images but also enhances watermark detectability, outperforming existing distortion-free methods. Our approach establishes a robust foundation for secure and trustworthy image synthesis, paving the way for more resilient watermarking mechanisms in future visual generation technologies.

References

- Scott Aaronson. 2022. [My AI safety lecture for UT effective altruism](#).
- Tom B Brown. 2020. Language models are few-shot learners. *arXiv preprint arXiv:2005.14165*.
- Miranda Christ, Sam Gunn, and Or Zamir. 2023. Undetectable watermarks for language models. *arXiv preprint arXiv:2306.09194*.
- Hai Ci, Pei Yang, Yiren Song, and Mike Zheng Shou. 2024. Ringid: Rethinking tree-ring watermarking for enhanced multi-key identification. In *European Conference on Computer Vision*, pages 338–354. Springer.
- Sumanth Dathathri, Abigail See, Sumedh Ghaisas, Po-Sen Huang, Rob McAdam, Johannes Welbl, Vandana Bachani, Alex Kaskasoli, Robert Stanforth, Tatiana Matejovicova, and 1 others. 2024. Scalable watermarking for identifying large language model outputs. *Nature*, 634(8035):818–823.
- Patrick Esser, Robin Rombach, and Bjorn Ommer. 2021. Taming transformers for high-resolution image synthesis. In *Proceedings of the IEEE/CVF conference on computer vision and pattern recognition*, pages 12873–12883.
- Pierre Fernandez, Guillaume Couairon, Hervé Jégou, Matthijs Douze, and Teddy Furon. 2023. The stable signature: Rooting watermarks in latent diffusion models. In *Proceedings of the IEEE/CVF International Conference on Computer Vision*, pages 22466–22477.
- Sam Gunn, Xuandong Zhao, and Dawn Song. 2024. An undetectable watermark for generative image models. *arXiv preprint arXiv:2410.07369*.
- Martin Heusel, Hubert Ramsauer, Thomas Unterthiner, Bernhard Nessler, and Sepp Hochreiter. 2017. Gans trained by a two time-scale update rule converge to a local nash equilibrium. *Advances in neural information processing systems*, 30.
- Micah Hodosh, Peter Young, and Julia Hockenmaier. 2013. Framing image description as a ranking task: Data, models and evaluation metrics. *Journal of Artificial Intelligence Research*, 47:853–899.
- Zhengmian Hu, Lichang Chen, Xidong Wu, Yihan Wu, Hongyang Zhang, and Heng Huang. 2023. Unbiased watermark for large language models. *arXiv preprint arXiv:2310.10669*.
- John Kirchenbauer, Jonas Geiping, Yuxin Wen, Jonathan Katz, Ian Miers, and Tom Goldstein. 2023. A watermark for large language models. *arXiv preprint arXiv:2301.10226*.
- Yuval Kirstain, Adam Polyak, Uriel Singer, Shahbuland Matiana, Joe Penna, and Omer Levy. 2023. Pick-a-pic: An open dataset of user preferences for text-to-image generation. *Advances in Neural Information Processing Systems*, 36:36652–36663.
- Rohith Kuditipudi, John Thickstun, Tatsunori Hashimoto, and Percy Liang. 2023. Robust distortion-free watermarks for language models. *arXiv preprint arXiv:2307.15593*.
- Tsung-Yi Lin, Michael Maire, Serge Belongie, James Hays, Pietro Perona, Deva Ramanan, Piotr Dollár, and C Lawrence Zitnick. 2014. Microsoft coco: Common objects in context. In *Computer vision—ECCV 2014: 13th European conference, zurich, Switzerland, September 6–12, 2014, proceedings, part v 13*, pages 740–755. Springer.
- Haotian Liu, Chunyuan Li, Qingyang Wu, and Yong Jae Lee. 2023. Visual instruction tuning. *Advances in neural information processing systems*, 36:34892–34916.
- Minjia Mao, Dongjun Wei, Zeyu Chen, Xiao Fang, and Michael Chau. 2024. A watermark for low-entropy and unbiased generation in large language models. *arXiv preprint arXiv:2405.14604*.
- Alec Radford, Jong Wook Kim, Chris Hallacy, Aditya Ramesh, Gabriel Goh, Sandhini Agarwal, Girish Sastry, Amanda Askell, Pamela Mishkin, Jack Clark, and 1 others. 2021. Learning transferable visual models from natural language supervision. In *International conference on machine learning*, pages 8748–8763. PMLR.
- Colin Raffel, Noam Shazeer, Adam Roberts, Katherine Lee, Sharan Narang, Michael Matena, Yanqi Zhou, Wei Li, and Peter J Liu. 2020. Exploring the limits of transfer learning with a unified text-to-text transformer. *Journal of machine learning research*, 21(140):1–67.
- Robin Rombach, Andreas Blattmann, Dominik Lorenz, Patrick Esser, and Björn Ommer. 2022. High-resolution image synthesis with latent diffusion models. In *Proceedings of the IEEE/CVF conference on computer vision and pattern recognition*, pages 10684–10695.
- Christoph Schuhmann, Romain Beaumont, Richard Vencu, Cade Gordon, Ross Wightman, Mehdi Cherti, Theo Coombes, Aarush Katta, Clayton Mullis, Mitchell Wortsman, and 1 others. 2022. Laion-5b: An open large-scale dataset for training next generation image-text models. *Advances in neural information processing systems*, 35:25278–25294.
- Jiaming Song, Chenlin Meng, and Stefano Ermon. 2020. Denoising diffusion implicit models. *arXiv preprint arXiv:2010.02502*.
- Quan Sun, Qiyang Yu, Yufeng Cui, Fan Zhang, Xiaosong Zhang, Yueze Wang, Hongcheng Gao, Jingjing Liu, Tiejun Huang, and Xinlong Wang. 2023. Emu: Generative pretraining in multimodality. *arXiv preprint arXiv:2307.05222*.
- Chameleon Team. 2024. Chameleon: Mixed-modal early-fusion foundation models. *arXiv preprint arXiv:2405.09818*.

- Ashish Vaswani, Noam Shazeer, Niki Parmar, Jakob Uszkoreit, Llion Jones, Aidan N Gomez, Lukasz Kaiser, and Illia Polosukhin. 2017. Attention is all you need. *Advances in neural information processing systems*, 30.
- Xinlong Wang, Xiaosong Zhang, Zhengxiong Luo, Quan Sun, Yufeng Cui, Jinsheng Wang, Fan Zhang, Yueze Wang, Zhen Li, Qiyang Yu, and 1 others. 2024. Emu3: Next-token prediction is all you need. *arXiv preprint arXiv:2409.18869*.
- Yi Wang, Yinan He, Yizhuo Li, Kunchang Li, Jiashuo Yu, Xin Ma, Xinhao Li, Guo Chen, Xinyuan Chen, Yaohui Wang, and 1 others. 2023. Internvid: A large-scale video-text dataset for multimodal understanding and generation. *arXiv preprint arXiv:2307.06942*.
- Yuxin Wen, John Kirchenbauer, Jonas Geiping, and Tom Goldstein. 2023. Tree-ring watermarks: Fingerprints for diffusion images that are invisible and robust. *arXiv preprint arXiv:2305.20030*.
- Yihan Wu, Zhengmian Hu, Hongyang Zhang, and Heng Huang. 2023. Dipmark: A stealthy, efficient and resilient watermark for large language models. *arXiv preprint arXiv:2310.07710*.
- Zijin Yang, Kai Zeng, Kejiang Chen, Han Fang, Weiming Zhang, and Nenghai Yu. 2024. Gaussian shading: Provable performance-lossless image watermarking for diffusion models. In *Proceedings of the IEEE/CVF Conference on Computer Vision and Pattern Recognition*, pages 12162–12171.
- Richard Zhang, Phillip Isola, Alexei A Efros, Eli Shechtman, and Oliver Wang. 2018. The unreasonable effectiveness of deep features as a perceptual metric. In *Proceedings of the IEEE conference on computer vision and pattern recognition*, pages 586–595.
- Xuandong Zhao, Prabhanjan Ananth, Lei Li, and Yu-Xiang Wang. 2023. Provable robust watermarking for ai-generated text. *arXiv preprint arXiv:2306.17439*.
- Chuanxia Zheng, Tung-Long Vuong, Jianfei Cai, and Dinh Phung. 2022. Movq: Modulating quantized vectors for high-fidelity image generation. *Advances in Neural Information Processing Systems*, 35:23412–23425.

A Missing Proofs

Theorem A.1. *Cluster-based reweight is distortion-free.*

Proof. We will show for all x , $\mathbb{E}_\theta[P_W(x|\mathbf{x}_{1:n}, \theta)] = P_M(x|\mathbf{x}_{1:n})$. Assuming w.l.o.g. $x \in c_1$, the probability of sampling x comes from two parts: a) $x \in c_{i'(\theta)}$ and b) $x \in c_{i''(\theta)}$.

Case 1. If $h \Pr(c_1) \leq 1$, as $c_{i'(\theta)}$ is uniformly selected from the cluster set, $\Pr(c_{i'(\theta)} = c_1) = 1/h$. Besides, the probability of sampling c_1 from the overflow distribution \mathcal{P}_c is 0. In this case,

$$\begin{aligned} \mathbb{E}_\theta[P_W(x|\mathbf{x}_{1:n}, \theta)] &= \Pr(c_{i'(\theta)} = c_1) \Pr(j < h \Pr(c_1)) \frac{P_M(x|\mathbf{x}_{1:n})}{\Pr(c_1)} \\ &= \frac{1}{h} * h \Pr(c_1) * \frac{P_M(x|\mathbf{x}_{1:n})}{\Pr(c_1)} \\ &= P_M(x|\mathbf{x}_{1:n}). \end{aligned} \quad (3)$$

Case 2. If $h \Pr(c_1) > 1$, we still have $\Pr(c_{i'(\theta)} = c_1) = 1/h$ and the probability of sampling c_1 from the overflow distribution \mathcal{P}_c is $\Pr_{c \sim \mathcal{P}_c}(c = c_1) := \frac{\min\{0, h \Pr(c_1) - 1\}}{\sum_{i=1}^h \min\{0, h \Pr(c_i) - 1\}}$. In this case

$$\begin{aligned} \mathbb{E}_\theta[P_W(x|\mathbf{x}_{1:n}, \theta)] &= \frac{1}{h} \Pr(j < h \Pr(c_1)) \frac{P_M(x|\mathbf{x}_{1:n})}{\Pr(c_1)} + \frac{1}{h} \sum_{i=2}^h \Pr(j > h \Pr(c_i)) \Pr_{c \sim \mathcal{P}_c}(c = c_1) \frac{P_M(x|\mathbf{x}_{1:n})}{\Pr(c_1)} \\ &= \frac{1}{h} \frac{P_M(x|\mathbf{x}_{1:n})}{\Pr(c_1)} + \frac{1}{h} \Pr_{c \sim \mathcal{P}_c}(c = c_1) \frac{P_M(x|\mathbf{x}_{1:n})}{\Pr(c_1)} \sum_{i=2}^h \Pr(j > h \Pr(c_i)) \\ &= \frac{1}{h} \frac{P_M(x|\mathbf{x}_{1:n})}{\Pr(c_1)} + \frac{1}{h} \Pr_{c \sim \mathcal{P}_c}(c = c_1) \frac{P_M(x|\mathbf{x}_{1:n})}{\Pr(c_1)} \sum_{i=1}^h \min\{0, 1 - h \Pr(c_i)\}. \end{aligned} \quad (4)$$

As $\sum_{i=1}^h \Pr(c_i) = 1$, $\sum_{i=1}^h \min\{0, 1 - h \Pr(c_i)\} = \sum_{i=1}^h \min\{0, h \Pr(c_i) - 1\}$, we have

$$\begin{aligned} \mathbb{E}_\theta[P_W(x|\mathbf{x}_{1:n}, \theta)] &= \frac{1}{h} \frac{P_M(x|\mathbf{x}_{1:n})}{\Pr(c_1)} + \frac{1}{h} \Pr_{c \sim \mathcal{P}_c}(c = c_1) \frac{P_M(x|\mathbf{x}_{1:n})}{\Pr(c_1)} \sum_{i=1}^h \min\{0, 1 - h \Pr(c_i)\}, \\ &= \frac{1}{h} \frac{P_M(x|\mathbf{x}_{1:n})}{\Pr(c_1)} + \frac{1}{h} \frac{P_M(x|\mathbf{x}_{1:n})}{\Pr(c_1)} \frac{\min\{0, h \Pr(c_1) - 1\}}{\sum_{i=1}^h \min\{0, h \Pr(c_i) - 1\}} \sum_{i=1}^h \min\{0, 1 - h \Pr(c_i)\}, \\ &= \frac{1}{h} \frac{P_M(x|\mathbf{x}_{1:n})}{\Pr(c_1)} + \frac{1}{h} \frac{P_M(x|\mathbf{x}_{1:n})}{\Pr(c_1)} (h \Pr(c_1) - 1), \\ &= P_M(x|\mathbf{x}_{1:n}). \end{aligned} \quad (5)$$

Combining Case 1 and 2, we can conclude that cluster-based reweight is distortion-free. \square